Tellus (1996), 48B, 234–253
Printed in Belgium – all rights reserved

TELLUS
ISSN 0280–6509

Influences on formation and dissipation of high arctic fogs during summer and autumn and their interaction with aerosol

By E. DOUGLAS NILSSON* and E. KEITH BIGG[1], *Department of Meteorology, Stockholm University, S-106 91, Stockholm, Sweden*

(Manuscript received 6 May 1995; in final form 31 August 1995)

ABSTRACT

Radiosondes established that the air in the near surface mixed layer was very frequently near saturation during the International Arctic Ocean Expedition 1991 which must have been a large factor in the frequent occurrence of fogs. Fogs were divided into groups of summer, transition and winter types depending on whether the advecting air, the ice surface or sea surface respectively was warmest and the source of heat. The probability of summer and transition fogs increased at air temperatures near 0°C while winter fogs had a maximum probability of occurrence at air temperatures between −5 and −10°C. Advection from the open sea was the primary cause of the summer group, the probability of occurrence being high during the 1st day's travel and appreciable until the end of 3 days. Transition fogs reached its maximum probability of formation on the 4th day of advection. Radiation heating and cooling of the ice both appeared to have influenced summer and transition fogs, while winter fogs were strongly favoured by the long wave radiation loss at clear sky conditions. Another cause of winter fogs was the heat and moisture source of open leads. Wind speed was also a factor in the probability of fog formation, summer and transition fogs being favoured by winds between 2 and 6 ms^{-1}, while winter fogs were favoured by wind speeds of only 1 ms^{-1}. Concentrations of fog drops were generally lower than those of the cloud condensation nuclei active at 0.1%, having a median of 3 cm^{-3}. While a well-defined modal diameter of 20–25 μm was found in all fogs, a second transient mode at about 100 μm was also frequently observed. The observation of fog bows with supernumerary arcs pointed to the existence of fog droplets as large as 200–300 μm in diameter at fog top. It is suggested that the large drops originated from droplets grown near the fog top and were brought to near the surface by an overturning of the fog layer. Shear induced wave motions and roll vortices were found to cause perturbations in the near-surface layer and appeared to influence fog formation and dissipation. The low observed droplet concentration in fogs limits their ability to modify aerosol number concentrations and size distributions, the persistent overlying stratus being a more likely site for effective interactions. It is suggested that variations in the fog formation described in this paper may be a useful indicator of circulation changes in the arctic consequent upon a global warming.

1. Introduction

The International Arctic Ocean Expedition 1991 (IAOE-91) was a joint ship operation (Anderson et al., 1991) of the Swedish ice-breaker *Oden*, the ice-breaking German research vessel *Polar Stern* and the U.S. coastguard ice-breaker *Polar Star*. On board *Oden* were the atmospheric programme together with the marine, technical and remote sensing programmes. The atmospheric programme of the IAOE-91 was designed to study the natural sulphur cycle and its climatological interactions (Leck et al., 1996), and included measurements and observations of marine chemistry and biology,

[1] Present address: 12 Wills Ave., Castle Hill, NSW 2154, Australia.
* Corresponding author.

atmospheric gas and aerosol particle chemistry, aerosol and cloud physics, boundary layer and transport meteorology.

One of the potentially important climatic feedback mechanisms is the melting of arctic ice resulting from global warming. This reveals water or land of a much lower albedo which enhances the surface warming if the skies are clear and the sun is well above the horizon. However, when the sun is substantially above the horizon the polar oceans are almost continuously covered with fog, low stratus or stratocumulus so that the albedo change resulting from melting will have a greatly diminished impact on the radiation budget. The fogs and cloud, too, may have strong impacts on air chemistry through providing an aqueous pathway for gas reactions and aiding the precipitation of particulates to the surface. For these reasons, we need to know what are the microphysical properties of the fog or cloud and the dominant mechanisms of their formation and dissipation. During the IAOE-91 it was not possible to sample the overlying cloud but with frequent surface meteorological observations, many radiosondes and 6-hourly air trajectories it was often possible to deduce the causes of fogs. Some measurements of their microphysical properties were also made.

Earlier works on the formation of fogs in the high Arctic are rare (Sverdrup, 1930a; Hansen, 1960) and concentrated on the advection fogs of the summer during June to August. Voskresensky (1969) and Kumai (1973) have studied drop size distributions in Arctic fogs, advection fogs above the mouth of the Ob' and north of the Gydan peninsula (73–74°N) in the region of Dikson Island and at Point Barrow (71°21′N) respectively, finding generally low to very low concentrations and relatively large drop sizes. These contrast strongly with drop size distributions in low arctic stratus measured from aircraft by Herman and Curry (1984), Curry and Herman (1985) and Brümmer et al. (1992). Droplet concentrations were much higher and modal drop sizes were usually smaller.

Curry et al. (1988) concluded that over the Beaufort Sea in June and July stratus or fog formed primarily as a result of isobaric cooling processes due to radiation and eddy diffusion. Once the stratus or fog became optically thick so that the radiative cooling became large, turbulent kinetic energy was produced and vertical mixing occurred. They found also that the occurrence of cloud was relatively insensitive to the sign of the large scale vertical velocity, attributing this in part to the humidity profiles. Humidity inversions were sometimes found above cloud top so that subsidence would actually transport moisture into the cloud. Curry (1986) also found that arctic stratus clouds occur in multiple layers, ranging from a surface fog underlying a stratus deck to 2 or more closely spaced cloud layers.

Curry and Ebert (1992) concluded that Arctic clouds have a net warming effect on the surface except around mid-summer. Radiative processes in the Arctic were examined by Vowinckel and Orvig (1962). More recent quantitative measurements have been made by Francis et al. (1991) in the Fram Strait summer Marginal Ice Zone (MIZ). Here it was found that the ice absorbed 40% less solar energy and 5% less IR energy than did the open water. However, the atmosphere over ice absorbed 6% more solar radiation and emitted 6% less IR than the open water resulting in a 1 K day^{-1} cooling over water compared to 0.86 K day^{-1} over ice.

On the IAOE-91 route, the ice in the MIZ during August was discoloured and had melt puddles of relatively low albedo, while north of about 85°N or closer to Greenland in September and at the return to the MIZ in October it was conspicuously cleaner. The typical contrast between ice and open leads would therefore probably have been somewhat greater than these figures would suggest. Francis et al. (1991) point out that the enhanced radiative cooling over water and relatively large heat fluxes into the atmosphere may cause destabilization of the layer near the surface.

Since the atmosphere actually warms in polar regions during summer in spite of the cooling effects of radiation, all writers have agreed that advection from the south must transport net heat and moisture into the region contributing to ice melting June through August. Herman and Goody (1976) have modelled the formation of fog and cloud in warm, moist air during advection over the melting pack ice with an internally consistent thermodynamic numerical model. They found that diffusive cooling and infrared cooling lowered the boundary layer temperature to condensation in less than 1 day after which a near-equilibrium of infrared boundary exchange and diffusion were established close to the surface. Including stability adjusted diffusivity they found that the intensity of mixing near the surface affected the altitude at which condensation first took place such that advection fog was formed the 1st and 2nd day and subsequently lifted during day 2 and 3 to form low stratus.

The ice begins to melt during May while advecting air is still below the ice melting temperature, due to increasing net radiation gain at the surface and continues to do so through most of September when the ice cover reaches its minimum extension before it starts to freeze again during winter. The seasonal transition in September and October, as freezing of the open leads and the first snowfall changes the albedo, involves relatively rapid temperature changes, on a time scale of a few days. These are caused by changes in the weather pattern as anti-cyclones formed over the ice are disturbed by cyclones from the south resulting in alternations between melting and freezing (Vowinckel and Orvig, 1970).

Nilsson (1996) described the arctic planetary boundary layer (PBL) during IAOE-91 as a stable

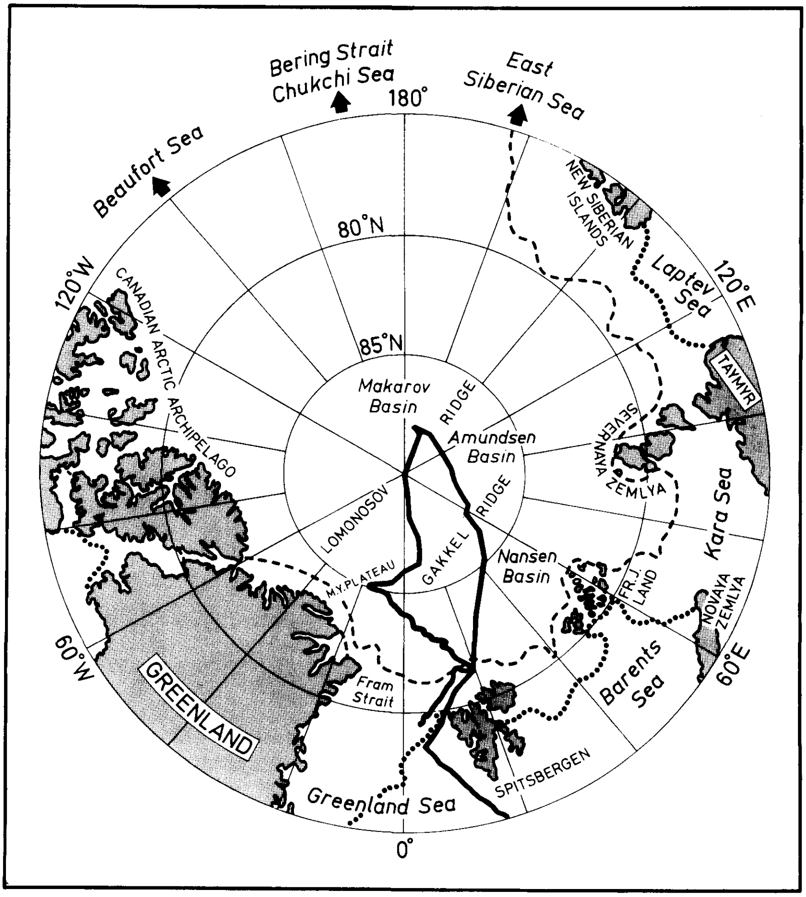

Fig. 1. Map of the Polar Ocean with maxima and minima ice cover between 1 August and 6 October 1991 and the cruise track of the ice breaker *Oden*. The cruise began in the Barents Sea on 1 August (Julian day 213). From August 4 to 7 (Julian day 216–219) *Oden* operated in open sea and the marginal ice zone west and north of Spitsbergen. During 10 days, *Oden* anchored in Isfjorden, Spitsbergen, for service, hence the break in data in some of the following figures. From 17 August (Julian day 229), *Oden* operated in the pack ice covered central Arctic ocean. On 5 October (Julian day 278), *Oden* reached open sea again in the Fram strait and the last station of the atmospheric programme took place in the Greenland Sea, October 6 (Julian day 279).

marine boundary layer (MBL) consisting of a mixed layer (ML) at the surface below a stable layer (SL) smoothly blending into the free troposphere. This model was appropriate for the stable MBL that still experienced cooling at the surface, since the ML was related to the existence of a low level jet (LLJ). It was also applicable to cases of weak convection when the ML increased in depth but the structure of a ML plus a SL remained. Most fogs observed during IAOE-91 took place in this ML, with the exception of pure radiation fogs, while the SL in general contained stratus and stratocumulus clouds.

It is clear from these works that advection, radiation changes and mixing of air with different properties are all likely to be important in arctic fog formation and that each of these processes may be involved in some fogs. We shall use statistics of fog formation together with other observations to try to decide which processes were dominant and describe the conditions favourable for formation or dissipation in the high Arctic during summer and fall. The influence of intermittent mixing in the stable MBL on fog formation or suppression and on the drop size distribution in fogs will also be considered. Since IAOE-91 lasted through August to October, this work will be able to compare the summer advection fogs found by Sverdrup (1930a) and Hansen (1960) with the fogs formed in September during the transition from summer to winter. Comparison will be made between the drop size distributions found during IAOE-91 and Voskresensky's (1969) and Kumai's (1973) drop size distributions and the potential for Arctic fogs to modify aerosol concentrations and properties and to participate in gas-to-particle conversions.

Finally, the importance of arctic stratus clouds and fog to climatic change will be discussed. All observations included took place in the permanent pack ice north of 80°N, on the route of the ice-breaker Oden shown in Fig. 1.

2. Methods

2.1. Meteorological observations

Observations of fog and visibility were made with the naked eye every hour or half an hour, about 30 m above sea level, simultaneously with observations of air temperature, water temperature, relative humidity, air pressure, cloud cover, cloud types, precipitation, relative wind speed and direction as well as ship speed and heading (Nilsson, 1996). Rawinsounding profiles from sondes launched from *Oden* of air temperature, relative humidity, pressure and winds have been used to evaluate the boundary layer structure and mixing processes during the IAOE-91 (Nilsson, 1996). Three-dimensional trajectories (McGrath, 1989) have been used together with ice maps to evaluate the time of advection over the pack ice from the open sea (Nilsson, 1996).

2.2. Ice temperature

The remote sensing programme of the IAOE 1991 performed drilling in the ice floes to achieve profiles (Carlström and Ulander, 1993). From their ice floe profiles of temperature, measured with a Fluke thermometer immersion probe, we have used the temperature at 5-cm depth as the approximate ice surface temperature (L.M.H. Ulander, personal communication).

2.3. Fog drop dize distribution

In the absence of more sophisticated equipment, a system of the greatest simplicity was used. A 60-mm diameter cardboard tube 50 cm long having removable end caps was saturated with water and left on deck until it had approximately reached ambient air temperature. Two circular glass microscope cover slips were thinly covered with silicone oil (DC200) by putting a drop between them, then sliding them apart. They were then also placed on the deck in covered containers. When cold, the tube's end caps were removed and it was pointed into the wind for 20 s, then inverted over a now-exposed cover slip in a vertical position and its top cap replaced. Fog drops within the tube were allowed 2 min to sediment out, the tube removed and the second cover slip placed lightly on top of the first. The cloud drops were then immediately examined with a microscope having a calibrated micrometer eyepiece.

The accuracy of the measurement depends on (1) water saturation being maintained in the tube, (2) diffusion of captured water drops into the oil or air spaces, (3) distortion of the captured drops and (4) turbulent losses to the walls when the tube was capped. The experimental procedure should have ensured that (1) provided no serious error. Droplets smaller than 15 μm diameter did shrink appreciably after capture and had to be measured and counted within 10 min for the diameters to be accurate. The penalty was a faster shrinking of the very small drops. These errors were probably less than those due to wall losses when the tube was capped and tilted. Because measurements were not made in high winds (too difficult keeping the tube vertical during cooling and sedimentation) it is unlikely that the errors were serious. The procedure should have caught 15 μm diameter and larger drops quantitatively but only half those of 10 μm diameter. Drops larger than 100 μm diameter were appreciably distorted by the overlying coverslip only if the oil was cold appearing larger than their true diameter. Measurements were therefore made in warm environment where the drops sank into the oil and were not distorted. No accurate independent checks were available. The absolute accuracy is not critical for the use we will make of the measurements, although comparison with earlier observations will be used to support satisfying accuracy.

2.4. *Radon*

Radon was estimated from the alpha-emitting decay products of radon attached to particles and caught on a filter. The method and its application during the IAOE-91 is decribed by Bigg (1996). Radon has a crustal origin. This means that it can be used as a tracer of continental air mass origin, but also as an indicator of vertical mixing since the radon consentration generally decreases from the surface and up.

2.5. *Condensation nuclei and cloud condensation nuclei*

Size distributions and concentrations of Condensation Nuclei (CN) in the size range 20 to 500 nm diameter were obtained using an electrostatic classifier (TSI Model 3071) and a TSI Model

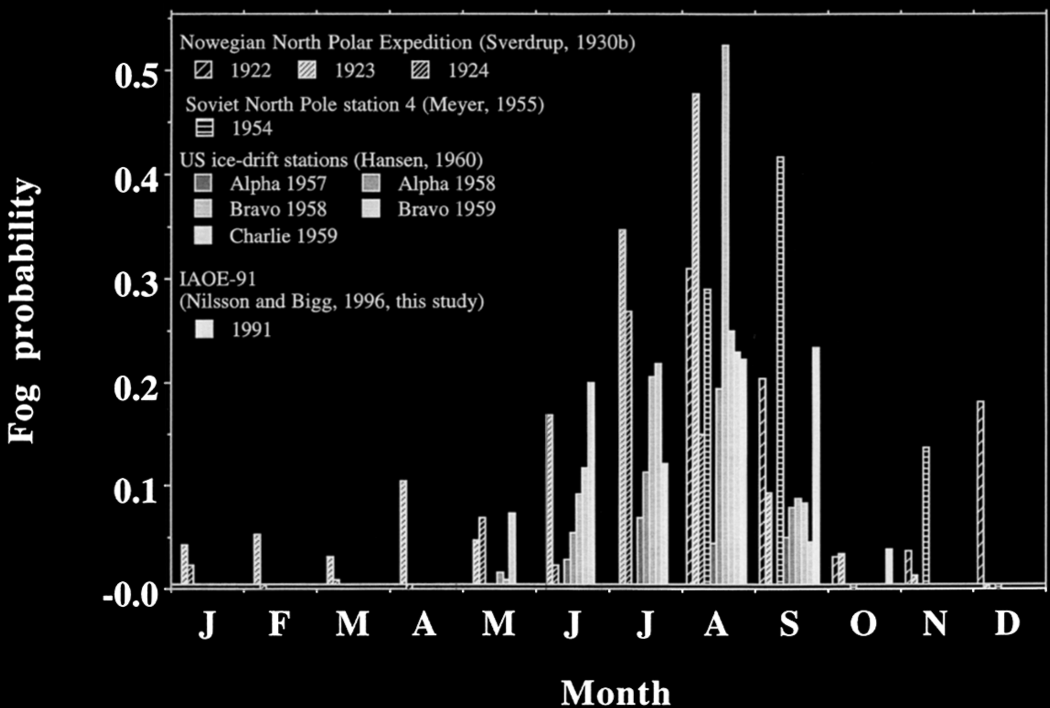

Fig. 2. The seasonal variation of the frequency of fog observations in the central Arctic ocean. Zero frequency is indicated with small columns below the *x*-axis. The observations made during the Norwegian north polar expedition before June 1923 did not distinguish between fog and haze so that the frequencies during winter are likely to be overestimations.

3760 CN counter. For a full description of these and associated measurements, see Covert et al. (1996).

Cloud condensation nuclei (CCN) concentrations were made using a continuous flow thermal diffusion chamber, the incomming air first being warmed to the top plate temperature, then brought to near water saturation before entering the chamber. Supersaturation was controlled by thermocoolers attached to the lower plate. Droplets larger than about 500 nm diameter were detected by a photocell as they left the chamber by forwardscattered light from a laser beam and recorded in one minute totals. Non-activated particles in this size range were found by the CN measurements to be rare north of latitude 80°N except on the few occasions when CN counts were high and should not usually have introduced serious errors. To avoid coincidence errors, only a small proportion of the droplets was counted, the correction factor being determined in the laboratory using monodisperse ammonium sulfate aerosols from an electrostatic classifier and a laser optical particle counter. The same system was used to check on the effective supersaturation which was somewhat lower than calculated. While the advection of particles with a critical supersaturation of 0.05 % was spread over a range of nominal supersaturations from 0.05 to 0.07 %, the concentration at the upper limit agreed to within about 30 % of the number expected from the correction factor. Accuracy improved at higher supersaturations in the laboratory but was almost certainly influenced at times on the ship by rapidly changing ambient temperatures or tilting of the ship.

3. Results and discussion

3.1. Seasonal variation

The seasonal variation of fog frequencies from observations performed during the IAOE-91 and earlier published observations are presented in Fig. 2. The summer months have the highest fog frequencies due to persistent fogs which cover large areas, but also high variation from season to season and from one region of the Arctic ocean to another, especially during the seasonal transition in September. The probability of fog in winter is low.

3.2. Formation of fogs in the high Arctic

3.2.1. Relative humidity in the lower atmosphere. A major difference between the lower troposphere over the arctic pack ice and that over land is the high frequency of humidities near water saturation. This is visualised in Fig. 3a where the frequency of humidities within 5 % and 10 % of water saturation is displayed against height normlised to the PBL top h′ (Nilsson, 1996). High values of relative humidity were naturally found within the stratus clouds of the Arctic MBL. In Fig. 3b is the frequency of humidities within 5 % and 10 % of water saturation displayed against height normalised to the ML height z_i. A minima is found in the ML between the fogs and the stratus clouds, although the frequency of near saturation is high within the entire ML. It is clear that quite small changes at the surface due to radiation cooling, mixing or moisture input could be sufficient to trigger fog

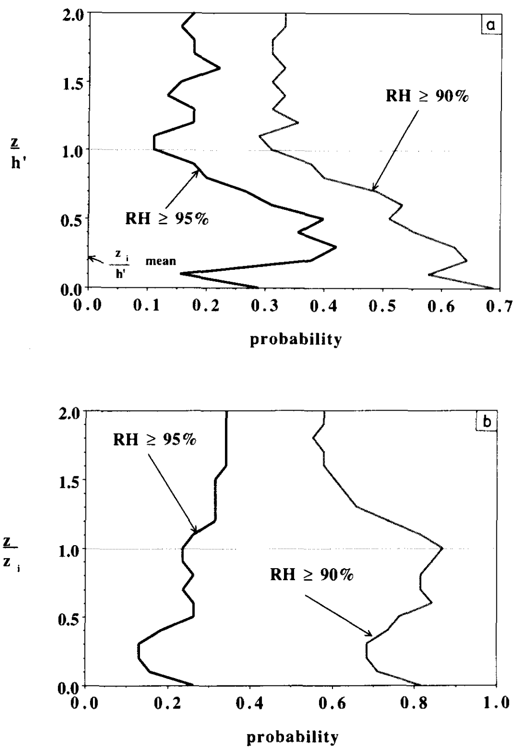

Fig. 3. The frequency of humidities within 5 % (full line) and 10 % (broken line) of water saturation against height normalised by (a) the PBL top h' and (b) the ML height z_i from radiosondes launched from *Oden* during the IAOE-91.

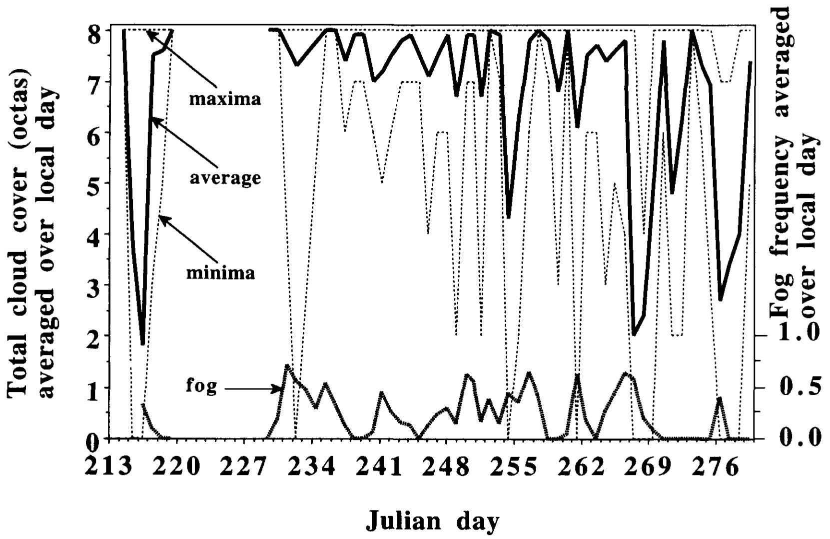

Fig. 4. Total cloud cover and fog frequency averaged over local days from observations performed from *Oden* during the IAOE-91.

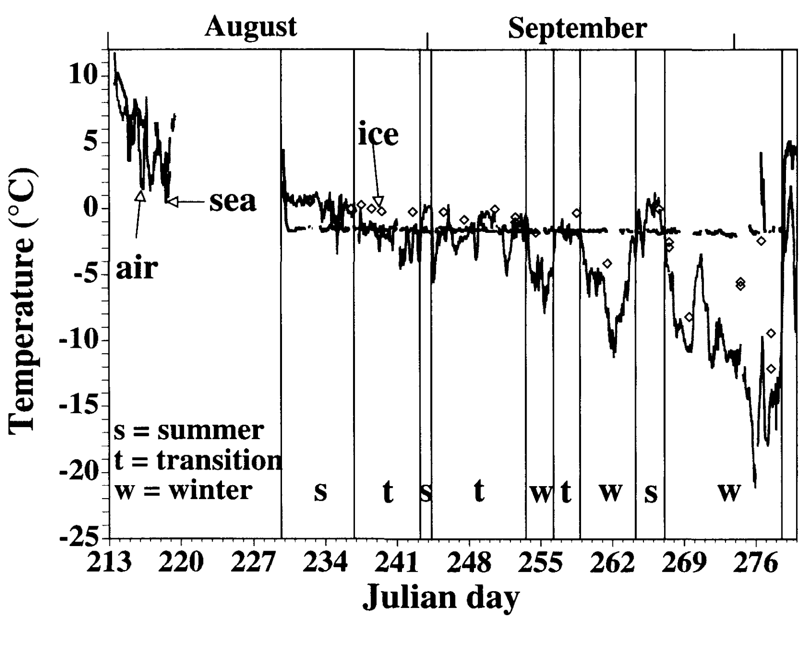

Fig. 5. Air (+30 m), sea surface (−3 m) and ice surface (−5 cm) temperatures during the IAOE-91. The periods defined to classify fog cases as summer, transition or winter while *Oden* was in the pack ice are marked.

formation. Several maxima in relative humidity (2–4 layers) were found within the PBL in about 50% of the relative humidity profiles, which confirms the multiple layer structure of arctic stratus clouds found by Curry (1986).

The cloud cover and fog frequency averaged over local days is presented in Fig. 4. The fog frequency has a high variability throughout the entire IAOE-91 with a lower frequency during the coldest periods in the end of the expedition. The cloud cover was near 8 octas during the first part of the expedition, while changes in temperature due to alterations in transport during the fall caused similar changes in cloud cover (Nilsson, 1996).

3.2.2. Temperature dependence. Air (at 30 m above surface), ice surface (at 5 cm depth into the ice) and sea (at 3 m depth) temperatures during the IAOE-91 are presented in Fig. 5. For the period that the ice breaker *Oden*, during the IAOE-91, spent in pack ice the temperatures of air followed a slow decline towards the winter with several large variations during fall on the time scale of days as warm air from the oceans and cold air aged over the ice cover alternated. The surface sea water temperature kept close to its freezing point. The surface ice temperature followed a seasonal decline similar to that of the air temperature, but delayed and with smoothed fluctuations such that the ice during transition periods was warmer than both the surrounding air and water.

A distinction can be made between cases where the advecting air, the ice/snow surface or the sea surface was warmer than the other two elements and hence the source of heat. We call the first group summer fogs since air temperature above the melting point of sea ice occur mainly during summer. The second group was called transition fogs since it represents the transition periods during the fall when heat stored in the ice floes allowed those to act as a source of heat. The last group was called winter fogs since occasions when the sea surface is the source of heat are typical for the winter. When there was no significant difference between the summer and transition fogs these were formed into one group and compared to the winter group to achieve better statistics. Since the temperatures were not known on all occasions the observations have been divided into nine continuous summer, transition and winter periods without following all fluctuations in temperature, see Fig. 5. Only observations made in above the pack ice of the central Arctic Ocean are included. In total, 1367 observations were performed north of the ice edge, 304 during the summer periods of Fig. 5, 445 during the transition periods and 598 during the winter periods. Fog was observed above the pack ice at in total 301 observations, 107 belonging to the summer group, 100 to the transition group and 94 to the winter group. Although earlier studies (Sverdrup 1930a, b; Hansen, 1960) covered several seasons, the size of this data set is comparable to these studies since observations were made more frequently.

The distribution of fog probability as a function of air temperature is shown in Fig. 6. The high probabilities of fog at temperatures near 0°C and −5 to −10°C and the low probabilities at −3 to −4°C suggest 2 entirely different processes of fog formation. The decreasing probability of fog at temperatures colder than −10°C is probably caused by the widening gap in relative humidity between water and ice saturation, leading to evaporation of water drops and sublimation of ice crystals on any exposed surface and hence increased erosion of water drops near the surface. Heavy growth of hoar frost occurred on all exposed surfaces when the relative humidity lay within this gap.

3.2.3. Transport. Other observations of the maximum in fog probability around 0°C are shown in Fig. 6. It was first observed by Sverdup (1930a) during June to August and later by Hansen (1960) during July to August, who attributed it to advection of warm moist air from open sea and the saturation of this air by cooling at the relatively colder surface of the pack ice covered sea. However as the air reaches the temperature of the surface no further formation of advection fog should take place, although the air would remain close to saturation. Therefore, advection fog ought to be dominant in the MIZ and at a distance into the pack ice, dependent on the initial air temperature, the surface temperature, the rate of advection and rate of heat loss at the surface. As can be seen from Table 1 where fog probability is listed as a function of transport time from the open sea, the group of summer fogs had their highest probability the first day after the

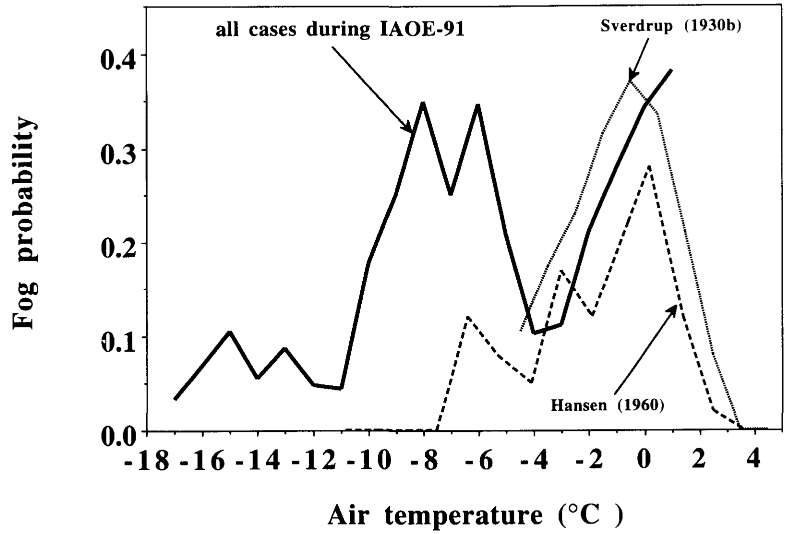

Fig. 6. The fog probability versus air temperature during the IAOE-91 and from the June through August months of the Norwegian North Polar expedition 1922–24 (Sverdrup, 1930b) and the July and August months of observations at the United States ice drift stations Alpha, Bravo and Charlie 1957-59 (Hansen, 1960).

ice edge and continued to occur to a lesser extent for 3 days. This time scale is supported by Herman and Goody's (1976) model of moist air from the open ocean transported over pack ice. The different course of probability of transition fogs with transport time suggests that other processes than cooling at the surface may have been important in their formation in air still close to saturation after a few days of advection. Possible causes are radiation, evaporation and intermittent boundary layer mixing and will be discussed below. The winter fogs appear to be entirely independent of transport time (probability between 0.2 and 0.3 during the first 4 days of transport over the ice) until the 5th

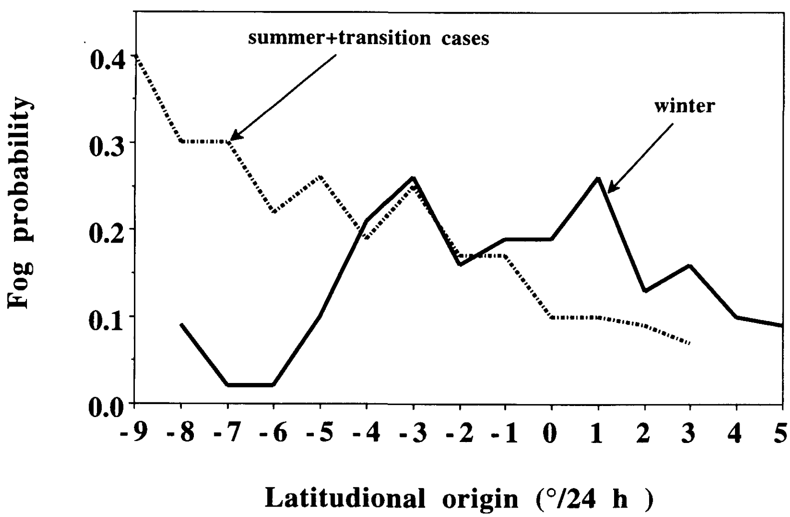

Fig. 7. Fog probability during the IAOE-91 versus latitudinal origin of air masses 24 h ago as revealed by trajectories.

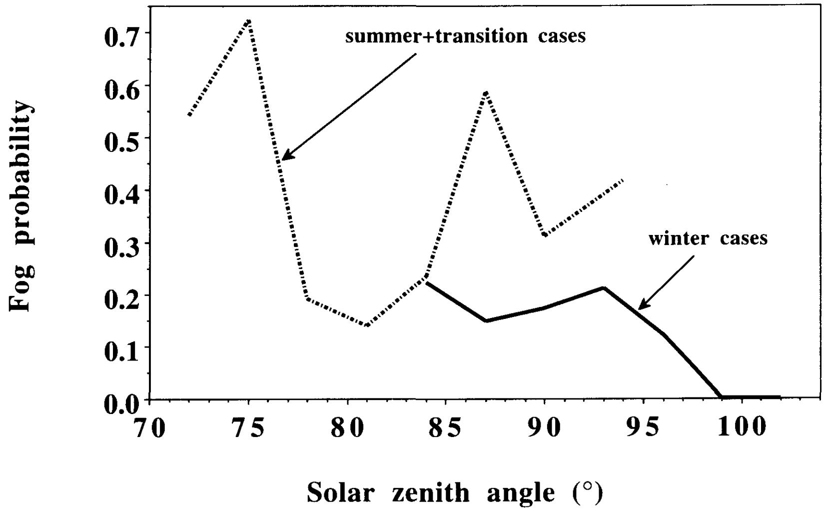

Fig. 8. The probability of fog against solar zenith angle during the IAOE-91.

day during which no fogs at all were observed, probably because the air after such a long time was too cold and too dry.

An alternative way to demonstrate the different transport dependence for the fog categories is presented in Fig. 7 where variations in fog probability with the latitude of the air 24 h earlier, obtained from trajectories, are plotted. It is obvious that speed of transport and an air mass origin in the south was an important factor in summer and transition fogs, but of less importance to the occurrence of winter fogs.

3.2.4. Solar radiation and cloud cover. Fig. 8 shows that radiation was also a significant factor in summer and transition fog formation. The high probabilities near the lowest solar zenith angles encounterd are consistent with enhanced moisture sources on the snow and ice from solar radiation near local noon. Indeed, relative humidity had a diurnal cycle and a mid day maxima. The dense and extensive stratus deck formed in the same air as the advection fogs is not likely to allow any diurnal variation in fog probability due to solar radiation. However the advection eventually leaves air and surface at equal temperatures no longer supporting formation of advection fog, but allowing the triggering of fog formation by the mixing of the slightly warmed and saturated air near the surface with overlying cold air near saturation. This is supported by the higher probability of summer fogs during the first days of advection while tran-

Table 1. *Probability of fog as a function of time since the air left open sea and entered the pack ice (Nilsson, 1996) for the first 5 days of advection during the IAOE-91; the groups of summer, transition and winter fogs have been separated.*

Fog group day	Summer + transition	Summer	Transition	Winter	All fogs
1	0.41	0.41	no cases	0.24	0.37
2	0.18	0.16	0.19	0.29	0.19
3	0.15	0.17	0.14	0.21	0.18
4	0.56	no cases	0.56	0.24	0.32
5	0.22	no cases	0.22	0.00	0.10

sition fogs dominated after a few days, as seen in Table 1. We interpret the maximum when the sun was near the horizon to be due to a resulting fall in air temperatures. Hansen (1960) who exclusively studied the advection fogs below the stratus cover of the summer found no significant diurnal variation in fog probability. Sverdrup (1930a) presented a minimum near local noon for the advection fogs while a midday maximum during some months of the autumn is hidden in the raw data (Sverdrup, 1930b).

Cloud cover was usually near 8 octas of stratus and almost never less than 5 when summer and transition fogs appeared and they showed no significant dependence on its changes. In strong contrast to this the group of winter fogs had a much higher probability of occurrence under clear skies (a probability of 0.68 for 0 octas of cloud cover) than in the presence of cloud cover (around 0.1 probability for 1–8 octas). This suggests that the winter group consisted of radiation fogs formed in the surface inversions caused by negative radiation balances below clear sky with the sun near or below the horizon. The open leads in the case of these fogs had been closed by new ice and eventually covered with snow, effectively isolating the air from the heat of the ocean (Liljequist, 1958; Overland and Guest, 1991). The group of winter fogs was less dependent on solar zenith angle than on cloud cover, so increased loss of long-wave radiation by decreased cloud cover appears to have been more important than decreased incoming short-wave radiation for the formation of radiation fog.

3.2.5. Wind speed dependence. During the periods shown in Fig. 5 when winter fogs were possible, leads of open water in the pack ice acted as sources of moisture and heat to the relatively cold air. This transfer of sensible and latent heat is known to be important in the Arctic Ocean winter since the flux is strongly dependent on thickness or non-existence of the ice (Maykut, 1978; Andreas et al., 1979; Andreas, 1980). This caused mixing fog, known as arctic sea smoke, which formed above the leads to become shallow and patchy fogs of a most local character that often drifted with the wind away from the lead or lifted from the surface to form stratus fractus clouds.

The probability of occurrence of these winter fogs was strongly dependent on wind speed as seen in Fig. 9, having a sharp peak at about 1 ms^{-1}. At

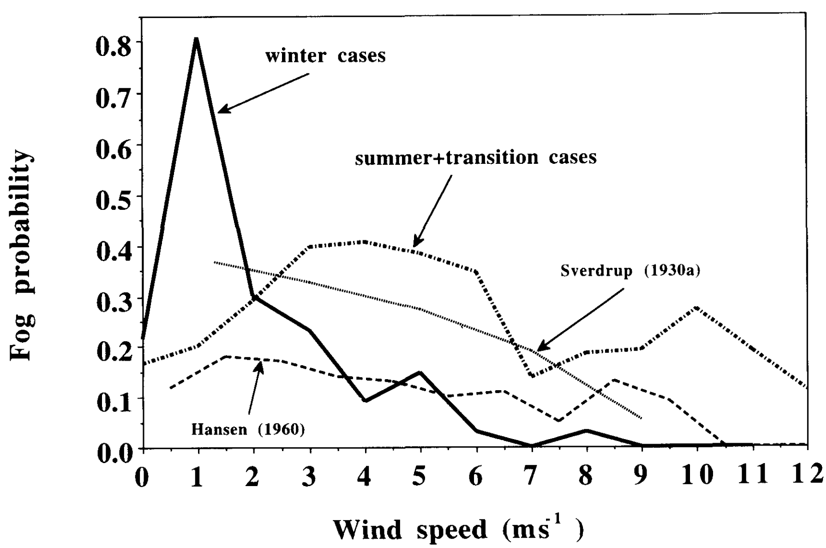

Fig. 9. The probability of fog against wind speed (at 34 m above the surface) during the IAOE-91 and from the June through August months of the Norwegian North Polar Expedition 1922-24 (Sverdrup, 1930b) and the July and August months of observations at the United States ice drift stations Alpha, Bravo and Charlie 1957-59 (Hansen, 1960).

higher wind speeds both mixing fog and radiation fog would be depleted due to too efficient turbulent heat transfer that would remove the gradients that are, in opposite ways, the basic cause of these fogs, while zero wind speed would allow the air and surface to reach temperature equilibrium again removing the cause of these fogs. Net loss or gain of radiation at the fog top may be of importance for the mixing fog.

Summer and transition fogs existed at wind speeds as high as 17 ms^{-1} but were favoured by wind speeds in the range 2 to 6 ms^{-1}, as seen in Fig. 9. Since the average surface wind speed was 6 ms^{-1} during the IAOE-91 (Nilsson, 1996) this ought to have made the summer and transition fogs sensitive to small changes in wind speed around the average. The existence of fogs at higher wind speeds suggests that the increased mixing that should follow with higher wind speeds was probably compensated by a stronger heat flux from the advecting air to the relatively colder surface as the fast advection sustained a large temperature difference. This is probably why the faster the air was transported from the south the higher was the fog probablity as seen in Fig. 7.

We can now conclude that the second maximum in fog probability at air temperatures between -5 and -10°C was caused by condensation due to radiation heat loss at the surface and/or mixing of cold air with the air slightly heated and saturated/almost saturated just above the water surface of leads causing radiation and mixing fogs (arctic sea smoke) respectively. Our best estimate is that radiation and mixing processes were of about equal importance for the formation of fogs in this temperature interval, possibly with some domination by radiation processes.

3.3. Size distributions of fog droplets

3.3.1. Mean drop size distributions. The mean overall drop size distribution during the IAOE-91 is shown in Fig. 10, each fog sampled being adjusted to an equivalent 100 droplets. The long tail of larger droplets in the distribution is misleading as it was only present in some of the samples whereas the 25 μm mode was present most of the time. For comparison, the size distribution found by Voskresensky (1969) for advection fogs near Dikson island, Russia, in July and Kumai (1973) for a "dense" persistent advection fog at Point Barrow, Alaska, in June is shown.

Droplet concentrations ranged from 0.3 to 10 cm^{-3}, with a median concentration of 3 cm^{-3}, considerably higher than in Kumai's "dense" fog of Fig. 10 (0.4 cm^{-3}) but comparable with the con-

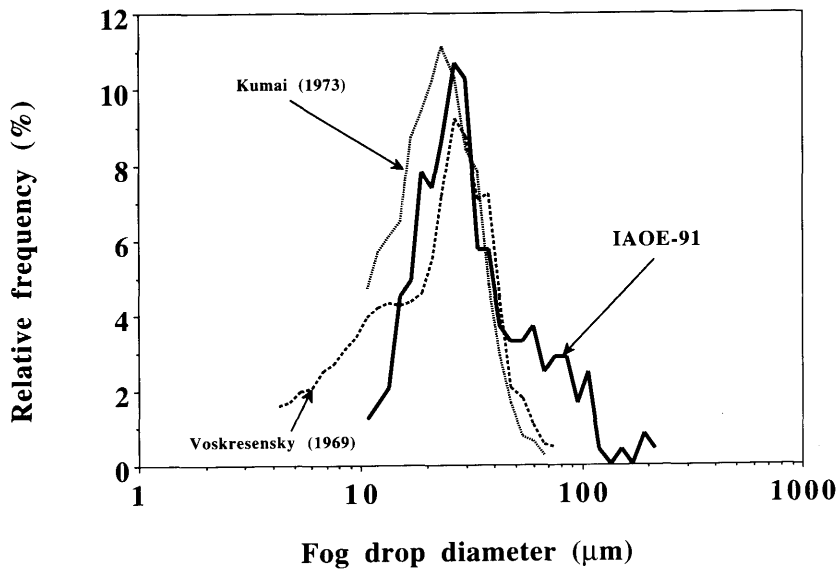

Fig. 10. Comparison of drop size distributions found by Voskresensky (1969), by Kumai (1973) and during the IAOE-91.

centrations he reported in other fogs where droplet sizes were smaller. At the times corresponding to the measurements used in this figure, CCN concentrations ranged from 30–80 cm^{-3} at 0.6% supersaturation and 7–20 cm^{-3} at 0.1%.

According to Silverman and Weinstein (1974) the daytime visibility V is given by:

$$V = \frac{3.912}{\pi \sum(K_i n_i r_i^2)},$$

where K_i is the scattering efficiency of the fog droplets (approximately 2), n_i is the droplet concentration and r_i the effective mean radius. Using metres as a unit, the relative frequencies of given radii determined from Fig. 10 and the median concentration of $3 \cdot 10^6$ m^{-3}, the visibility from the above formula turns out to be 430 m, which was typical of those observed. Visibility is defined as the distance at which a black target can just be detected against a horizon sky with contrast threshold of 2%. In the high Arctic, with grey skies, low solar elevations and an almost completely white foreground the visual estimate may well depart from the above formula and the most we can claim is that droplet size distributions and visibilities are consistent within the wide probable errors of the latter.

3.3.2. Reasons for low droplet concentrations. With advection fogs, the main reason for low concentrations is likely to be the very slow changes relative to the environment as the air advected. When saturation is reached, it is exceeded so slowly that very few growing droplets are needed to prevent further rise in relative humidity. In cases where the open leads were appreciably warmer than the air, supersaturations and initial droplet concentrations above the sources would probably have been much higher. Observed droplet concentrations in fogs of this type were all about 1 cm^{-3} or less, probably because the fog initiated over the leads was diluted by mixture with fog free but nearly saturated air as it drifted over the ice floes. In such cases only a small fraction of the total aerosol would have been involved in condensation but the sizes involved may have extended down to those active at supersaturations perhaps as high as 1% because of the vigorious mixing above the relatively warm water.

3.3.3. Evolution of large drops. Changes in visibility over periods of 30–90 min were fairly obvious during persistent fogs as was the intermittent fall-out of drops having terminal velocities of tens of cms^{-1} and the reason for the changes was revealed by successive drop size distributions. An

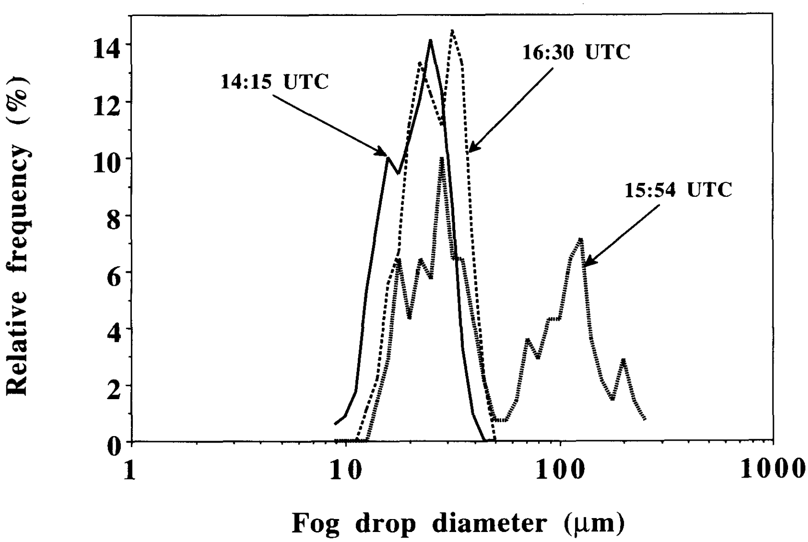

Fig. 11. Sudden changes in drop size distribution during a fog on 20 August (Julian date 232) during the IAOE-91.

example is shown in Fig. 11 of a fog which began just before 14 UTC, 20 August 1991 (Julian date 232). The first, 15 min after the onset, showed a narrow drop size distribution and a concentration of 10 cm^{-3}, typical for the advection fogs of the summer periods and much higher than in subsequent colder fogs (the air temperature was between 0 and 1°C). Larger droplets appeared about an hour and a half later (shown in the 15:54 UTC distribution) and remained in evidence for about 30 min together with a reduced population of the original distribution. However, the fog had returned to its original size distribution by 16:30 UTC. On other occasions, large droplets dominated the distribution within 40 minutes. Sudden appearance of larger droplets like those in Fig. 11 formed the tail of the size distribution in Fig. 10. Similar sudden appearances of larger droplets were found by Voskresensky (1969). The largest drops of the size distribution's upper tail were observed to grow from 60 μm to 80 μm in 20 minutes while the 20–25 μm mode decreased, and those from 80 μm to 210 μm in diameter within 30 minutes. Kumai (1973) in the most extreme case observed the largest drops of the tail to grow from 50 μm to 130 μm in 10 min.

The fairly consistent modal diameter of 25–30 μm probably represents the limit achieved by condensational growth under the conditions of very low drop concentration and temperatures near or below 0°C. The transient secondary mode seen in Fig. 11 had a comparable frequency of droplets centred around 100 μm diameter. For droplets of this size to have formed in as little as 40 min when concentrations were so low some mechanism for enhancing coalescence must have been present. One possible explanation is an "accumulation zone" of higher droplet concentrations near the fog top where net upward motions cease. If the large drops formed there by coalescence simply fell out from a steady state fog we would not expect such a noticeable population of large droplets near the surface. Instead it suggests that the accumulation of larger drops in the upper part of the fog was suddenly transferred to near the surface. An overturning of the fog layer could achieve this, or a suppression of the upward motions by the larger drops that had formed. Aircraft observations by Voskresensky (1969) indeed found a greater proportion of large droplets at the fog top. His Fig. 1 shows probabilities of 25, 50 and 100 μm droplets to be respectively 1.0, 2.3 and 2.6 times as great at fog top as at fog bottom.

3.3.4. Ice crystals. The fogs described here were with few exceptions water fogs. Ice crystal which actually originated in a fog were observed only once, in the beginning of October, at a temperature of -18°C and were only of the order of 10^{-3} to 10^{-2} cm^{-3} when they had become large enough to be visible. In fogs at warmer temperatures ice crystals in similar concentrations were noted on several occasions but their crystal habit showed that their growth had occured at lower temperatures in the overlying clouds. It is unlikely that melted ice crystals were responsible for the larger droplets, like those in Fig. 11, since ice crystals that reached the surface were always several mm in diameter and, if melted would have produced drops far larger than those observed. Concentrations were also usually several orders of magnitude less than concentrations of large droplets.

3.3.5. Optics in arctic fogs: the white fog bow. When the sky above the winter fogs was clear, fog bows were observed. Arctic fog bows are known from the Norwegian North polar expedition described as "white arc opposite to sun" (Sverdrup, 1930b). During the Norwegian North polar expedition the fog bow was observed on eleven occasions from 1922 to 1924, ten of them in the summer months, June to September, usually in fogs below clear or almost clear sky and always opposite the source of light (usually the sun, but for one of the observations the moon). The radius of the fog bow was estimated to be about 40° for one of the observations. During the IAOE 1991, the fog bow, or part of it, was observed three times during September in fogs below 0 to 3 octas of cloud cover. The most brilliant of these fog bows, which was observed above a mixing fog with a sharp fog top, is shown in Fig. 12. For this fog bow, the maxima in the intensities of the three distinguishable bows were measured to be 42.3°, 36.7° and 33° identified as the primary arc, the first supernumerary arc and the second supernumerary arc. The supernumerary arcs are caused by interference between light on both sides of the angle of minimum deviation in the drops that cause the primary bow, and by the distortion of larger drops which moves the maximum light intensity of the larger drops away from the minimum of the

Fig. 12 Photographic picture of a mixing fog and a white fog bow with supernumerary bows observed during the IAOE-91 on 11 September (Julian date 254).

smaller drops (Fraser, 1983). It is unusual to see anything but a faint first supernumerary bow. The supernumerary bows observed from *Oden* allow the possibility of estimating the size of the drops that caused the fog bow. The drops had to be smaller than rain drops to give wide bows with colours mixed to white. To give the high intensity and more than one supernumerary bow many of the drops had to be between 200 and 300 μm (Fraser, 1983). Drops of that size, more or less drizzle, are in the upper tail of the size distribution of Fig. 10 and were only occasionally observed. Hence the supernumerary arcs of the fog bow are only likely to show up during events of drizzle precipitation in fog given the right light conditions. Such events are likely to last for a limited time. It might be that the three hour duration and the presence of supernumerary arcs in the fog bow of Fig. 12 are uncommon.

The important point is that the supernumerary arcs confirmed the existence of drops as large as 200 μm diameter at the fog top and the clear sky above proved that they could not in this case have been drizzle from clouds but must have grown within the fog.

3.4. *Influences of intermittent and/or organised PBL mixing*

If a fog has a vertical gradient in droplet size distribution such as larger drops at the fog top, overturning of the fog layer by a sudden enhanced mixing would bring an influx of drops from the fog top to the fog bottom. This would cause the appearance of a transient mode of larger droplets such as that shown in Fig. 11. The overturning could arise from radiational changes at the fog top and/or from shear induced wave motions in the presence of a low-level jet. Such wave motions (Cheung, 1991; Walter and Overland, 1991; Nilsson, 1996) and LLJs (Shapiro and Fedor, 1986, Brümmer et al., 1994, Nilsson, 1996) have recently been observed in the arctic PBL. A radiosonde was launched from *Oden* at 16:11 UTC between the 2nd and the 3rd size distributions of Fig. 11. From analysis of the profiles of virtual potential temperature, wind speed and direction and Richardson number, see Fig. 6a of the companion paper by Nilsson (1996), the radiosonde revealed the presence of an LLJ with layers of critical Richardson numbers that may have housed shear induced Kelvin–Helmholtz (K–H) waves or gravity waves. If the K–H wave was breaking, the fog layer would be mixed, which could result in the observed sudden change in droplet size distribution. Interactions between a fog and gravity waves have been observed by Duynkerke (1991).

Although the formation of fogs in the Arctic may be understood statistically, as attempted above, the experience remains that these fogs may clear even during the most favourable conditions or appear under unfavourable conditions, sometimes accompanied by sudden changes in temperature. Intermittent mixing within the stable MBL caused by shear induced waves in the presence of LLJ:s may not only cause sudden changes in droplet size distribution but may also trigger the formation or clearing of fog in air close to condensation/evaporation. The LLJ and associated wave motions were commonly present during IAOE-91 (Nilsson, 1996) and they have been demonstrated to cause sudden concentration changes in tracers like radon and aerosol or in aerosol size distribution (Bigg et al., 1996).

The interaction between turbulence, radiative transfer and cloud microphysics suggested by Curry (1986) and the possible interaction between radiation; fog/cloud drop condensation/evaporation; aerosol number and number size distribution; and boundary layer stability and mixing suggested by Bigg et al. (1996) appear to be essential to an understanding of the arctic atmosphere. It should be studied by simultaneous observations of turbulence and cloud and aerosol physics with as high time resolution as possible.

Fig. 13 shows a long sequence of oscillations in radon with a period of about 100 minutes on August 23 (Julian date 235) at latitude 85° N. The sudden radon jump at Julian day 235.2 corresponded to a change in air mass, according to trajectories arriving at the surface, from air that had circulated over the pack ice at high latitudes to air that had been over open water. The accompanying advection fog ended in a flurry of relatively large drops at a time of radon minimum. This minimum should, if radon decreased with height, have corresponded to a down mixing of air and an over-

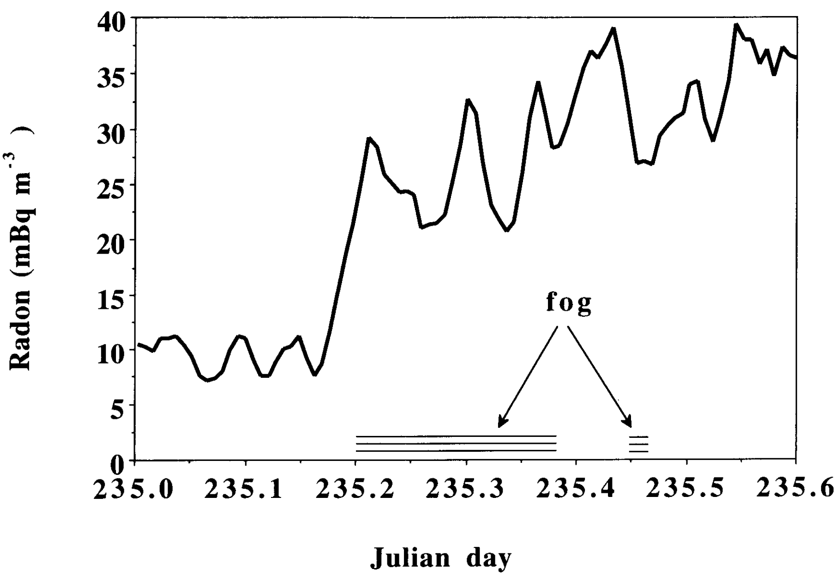

Fig. 13. Periodic variations in radon and observations of fog on August 23 (Julian date 235) during the IAOE-91.

turning of the fog. Periodicities in radon have been associated by Bigg et al. (1996) with roll vortex circulations described by Nilsson (1996). A radiosonde launched later the same day supported the existence of roll vortices. It is possible that this fog was overturned and dissipated by the down-draft in roll vortices.

Repeated fog formation and clearing was observed at other occasions of roll vortex circulations like in the roll vortices of 12 September (Julian date 255) described in detail in a companion paper (Nilsson, 1996). If this influence on fogs had been noticed during the expedition more cases of sudden precipitation in fogs and repeated formation and clearing of fog associated with secondary circulations would probably have been documented. Since the period of the rolls usually was close to the observation interval we can however now only speculate that the up-draft and down-draft in roll vortices may be of great importance for condensation and evaporation in fog as well as cloud. Walter and Overland (1984) have observed fog streets, over the winter ice of the Bering Sea February to March 1983, associated with roll vortices. Since the axis of roll vortices are tilted in relation to the geostrophic wind the up-draft (saturated) and down-draft (undersaturated) regions of the roll vortices move across a fixed point at the surface. We suggest that fog streets like those observed by Walter and Overland (1984) caused the repeated fog formation and clearing observed during the IAOE-91.

3.5. *Interaction of fog and aerosol*

The low concentrations of both aerosol and fog droplets means that Brownian capture of aerosol by droplets will be very slight. The large droplets may catch some particles by impaction but again their rarity and the inefficiency of the process will make this an infrequent event. The greatest losses have to be through nucleation followed by fall-out, which fog observations suggest to take from 40 to 90 min. The losses due to nucleation and the possibility of release of many of the nuclei when the fog evaporates has been examined by considering mean aerosol concentration changes near the onset and end of fogs. There is a problem in defining the onset of fog because the presence of absence of fog was recorded only at half-hourly or hourly intervals. Arbitrarily onset is taken to be 10 min before the first observation of fog and its end ten minutes after the last. Because mean concentrations varied by a large factor between fogs, to give them all equal weight it is necessary to

Table 2. *Relative mean aerosol concentrations near the start and end of fogs lasting at least 90 min from observations during the IAOE-91*

Time	Number concentration (cm^{-3})			
Min from start	CN > 41 nm	CN > 206 nm	CCN (0.63%)	CCN (0.05%)
−30	108	101	109	120
−20	112	109	103	106
−10	100	103	96	91
0	97	105	97	90
10	94	90	96	93
20	97	95	99	97
30	94	96	100	103
Min from end				
−30	92	94	96	85
−20	95	95	95	85
−10	100	106	92	88
0	103	100	94	92
10	99	107	99	95
20	103	101	109	105
30	114	109	118	118

express particle concentrations as a percentage of the mean for the particular fog. The periods considered are from 30 min before onset to 30 min after and 30 min before end to 30 min after. In each interval the mean normalized concentration was calculated for all persistent fogs for which unbroken particle records were available. The result is shown in Table 2 for CN > 41 nm and > 206 nm diameter and for CCN at 0.63 % and 0.05 % supersaturation. If all particles were composed wholly of ammonium sulfate, the CN > 41 nm and CCN at 0.63 % or CN > 206 nm and CCN at 0.05 % would be identical.

There appear to be a significant mean decrease of about 15–25 % at the onset of the fogs and a restoration at the end of the fogs, but there is no way of deciding whether this is due to the changes in air history that accompany these events or to the formation or evaporation of the fog droplets. Once the fog was established there seems to have been very little mean subsequent loss. Both decreases and increases in aerosol concentrations were observed, although on average it was a decrease.

In summary, it seems that the fogs, especially the mixing and radiation fogs during winter conditions and in air aged several days over the pack ice, must be relatively inefficient vehicles for particle removal simply because of their low droplet concentrations. More of this action will occur in the denser and more persistent advection fogs, during summer and the first days of advection over the ice, and presumably much more in the denser and far more persistent overlying stratus. Fall-out and evaporation of droplets from these clouds may provide many of the nuclei for fog formation.

4. Fog and cloud observations and climatic change

Many general circulation models, used to predict climatic change through the influence of added atmospheric carbon dioxide have included a positive feedback term involving the melting of polar pack ice. The argument is that during the period when the sun is above the horizon, the ice reflects a high proportion of the energy back to space. If rising temperatures cause more of the dark ocean to be exposed, less radiation is lost and the warming enhanced.

Our own observations, as well as those of earlier observers, show that during the summer season when the sun is high enough to have an appreciable energy input, the arctic and antarctic pack ice areas are almost permanently shrouded by multiple layers of stratus and stratocumulus and very frequently by fog as well. It may not primarily be the melting of the ice that alters the albedo, but the extent of cloud cover and its albedo.

We therefore need to ask such questions as the following.

(1) There are probably not long enough and continuous enough series of soundings above the central Arctic Ocean to identify any trends in the PBL structure and stability. However, a decrease in surface air temperature and a decline in inversion depth, related to warming by greenhouse gases, in the North American Arctic for the past 20 to 30 years have recently been found by Bradley and Keimig (1993) for the winter months. Would a similar decrease in the stability of the central Arctic Ocean PBL during the spring, summer and fall due to greenhouse warming be accompanied by a decrease in formation of stratus and fog?

(2) Will altered atmospheric circulations, introduced by climate changes, increase or decrease the advection of warm air from the south above the Arctic ocean and in this way change the PBL stability?

(3) Will such changes extend or limit the period (June through August) during which advection dominates the ice melting and stratus and fog formation and limit or extend the periods (May and September) during which the net gain of solar radiation at the ice surface melts the ice cover?

(4) How will such changes influence the stratus and fog formation in air that has been aged a few days over the ice and reached a near-equilibrium with close to condensation conditions? It may be that condensation/evaporation in such air is especially sensitive to stability changes, while changes in transport regimes may alter the extent of the influenced areas.

(5) Will the transport and local summer aerosol production in polar regions be altered by greenhouse warming and how will this change the albedo and optical thickness of clouds?

While the present expedition could not hope to answer those questions, the way in which fog occurrence was dependent on various factors in 1991 may perhaps form the basis for rather sensitive indications of changes that have happened subsequently.

5. Conclusions

We have seen that during IAOE-91 the fogs that occurred were conveniently separated into three categories related to the heat and vapour exchange between surface. When this was done, consistent descriptions of some of the influences causing the different types of fog resulted. The mechanisms of fog formation and the nature of the influences suggested by these descriptions were in broad agreement with earlier work on arctic summer advection fogs, but were perhaps indicated more clearly. The seasonal transition between summer and winter was associated with a high sensitivity in the fog, and probably stratus, formation dependent on small and intricate changes in the environment such as radiation balance, stability and turbulent mixing. For the high arctic late fall and probably winter, arctic sea smoke and radiation fogs were identified as the dominant fog types. The drop size distributions, 25 μm diameter modal drop size and concentrations of droplets were again consistent with earlier work but showed the transient nature of a mode of large droplets centred around 100 μm diameter. The most likely explanation of the sudden appearances and disappearances of this mode is that turbulent mixing related to shear induced wave motions caused a destabilization and overturning of the fog layer. The same explanation was found to be essential for frequent sudden and often very large changes in aerosol concentrations and size distributions that form the subject of a companion paper (Bigg et al., 1996). The possibility that roll vortices were also involved in fog formation and dissipation, as they appeared to have been in the case of rapidly changing aerosol concentrations, is an obvious field for further study. Continuous monitoring of fog size distributions would not be too difficult an exercise on a future expedition and might add considerably to detection and understanding of sudden mixing events.

The often critical balance between fog and no-fog situations revealed in this paper suggests that global warming may significantly alter the frequency of fog formation. It is reasonable to suspect a similar sensitivity of stratus formation in the arctic stable MBL. Comparison of probability of fog formation with those described in this paper might provide a sensitive indication of meteorological/climatological changes in the intervening period. Changes in the probability of fog, or stratus, formation and areal extent may be important also because they modify the ice-sea albedo change consequent upon warming which is usually included in general circulation models of climate change.

6. Acknowledgements

We thank the officers, the crew and our fellow scientists on board the ice breaker *Oden* for their assistance and cooperation making the expedition so successful. We thank everyone who, in addition to the meteorologists of the atmospheric programme, took part in the weather observations. We thank M. Westin, now at the Weather Service of the Swedish Airforce, for good and hard work during the expedition. This research was founded by contract number E-EG/GU 9906-30, E-EG 3922-313 of the Swedish Natural Science Research Council and by the Knut and Alice Wallenberg Foundation.

REFERENCES

Anderson, L., Lönnroth G. and Carlsson, M. (editors), 1991. Swedish Arctic Research Programme 1991, International Arctic Ocean Expedition 1991: Icebreaker *Oden*: *A cruise report*. Swedish Polar Research Secretariat, P.O. Box 50005, S-104 05 Stockholm, Sweden.

Andreas, E. L. 1980. Estimation of heat and mass fluxes over Arctic leads. *Mon. Weather Review*, **108**, 2057–2063.

Andreas, E. L., Paulsson, C. A., Williams, R. M., Lindsay, R. W. and Bussinger, J. A. 1979. The turbulent heat flux from Arctic leads, *Boundary Layer Meteorology*, **17**, 57–91.

Bigg, E. K. 1996. Ion induced nucleation around radon daughters in remote arctic maritime air. *Tellus* **48B**, this issue.

Bigg, E. K., Leck C. and Nilsson, E. D. 1996. Sudden changes in arctic atmospheric aerosol concentrations during summer and autumn. *Tellus* **48B**, this issue.

Bradley, R. S. and Keimig, F. T. 1993. Recent changes in the North American Arctic boundary layer in winter. *J. Geophys. Res.*, **98**, D5, 8851–8858.

Brümmer B., Rump, B. and Kruspe, G. 1992. A cold air outbreak near Spitsbergen in springtime-boundary layer modification and cloud development. *Boundary Layer Meteorol.* **61**, 13–46.

Brümmer, B., Busack, B., Hoeber, H. and Kruspe, G. 1994. Boundary-layer observations over water and Arctic sea-ice during on-ice air flow. *Boundary-Layer Meteorol.* **68**, 75–108.

Carlström, A. and Ulander, L. M. H. 1993. C-band backscatter signatures of old sea ice in the central Arctic during Freeze-up. *IEEE Transactions on Geoscience and Remote Sensing* **31**, 4, 819–829.

Cheung, T. K. 1991. Sodar observations of the stable lower atmospheric boundary layer at Barrow, Alaska. *Boundary-Layer Meteorol.* **57**, 251–274.

Covert, D. S., Wiedensohler, A., Aalto, P., Heintzenberg, J., McMurry, P. H. and Leck, C., 1996. Aerosol number size distributions from 3 to 500 nm diameter in the arctic marine boundary layer during summer and autumn. *Tellus* **48B**, this issue.

Curry, J. A. and Herman, G. F. 1985. Infrared properties of summertime Arctic stratus clouds. *J. Clim. Appl. Met.* **24**, 525–538.

Curry, J. A. 1986. Interactions among turbulence, radiation and microphysics in the Arctic stratus clouds. *J. Atm. Sci.* **43**, 90–106.

Curry, J. A., Ebert, E. E. and Herman, G. F. 1988. Mean and turbulence structure of the summertime Arctic cloudy boundary layer. *Quart. J. Roy. Met. Soc.* **114**, 715–746.

Curry, J. A. and Ebert, E. E. 1992. Annual cycle of radiative fluxes over the Arctic Ocean: sensitivity to cloud optical properties. *J. Clim.* **5**, 1267–1280.

Duynkerke, P. G. 1991. Observations of a quasi-periodic oscillation due to gravity waves in a shallow radiation fog. *Quart. J. Roy. Met. Soc.* **117**, 1207–1224.

Francis, J. F., Ackerman, T. P., Katsaros, K. B., Lind R. J. and Davidson, K. L. 1991. A comparison of radiation budgets in the Fram Strait summer marginal ice zone. *J. Climate* **4**, 218–235.

Fraser, A. B. 1983. Chasing rainbows. *Weatherwise* **36**, 280–289.

Hansen, D. C. 1960. *Forecasting summer fog in the central Arctic.* M.Sc. thesis, University of Washington, Seattle, WA, USA.

Herman, G. and Goody, R. 1976. Formation and persistence of summertime Arctic stratus clouds. *J. Atm. Sci.* **33**, 1537–1553.

Herman, G. F. and Curry, J. A. 1984. Observational and theoretical studies of solar radiation in Arctic stratus clouds. *J. Clim. Appl. Met.* **23**, 5–24

Kumai, M. 1973. Arctic fog droplet size distribution and its effect on light Attenuation. *J. Atm. Sci.* **30**, 635–643.

Leck, C., Bigg, E. K., Covert, D. S., Heintzenberg, J., Maenhaut, W., Nilsson E. D. and Wiedensohler, A. 1996. Overview of the Atmospheric research program during the Interational Arctic Ocean Expedition of 1991 (IAOE-91) and its scientific results. *Tellus* **48B**, this issue.

Liljequist, G. H. 1958. Long-wave radiation and turbulent heat transfer in the Antarctic winter and the development of surface inversions. *Polar Atmosphere Symposium, Part 1, Meteorology Section*, ed.: Sutcliffe, R. C. AGARD-NATO Symposium, Oslo, 2–8 July 1956.

Maykut, G. A. 1978. Energy exchange over young sea ice in the central Arctic. *J. Geophys. Res.* **83**, C7, 3646–3658.

McGrath, R. 1989. *Trajectory models and their use in the Irish Meteorological Service.* Memorandum no. 112/89, Irish Meteorological Service, Dublin.

Meyer, H. K. 1955. Das Wetter der Nähe des Nordpols. *Meteorologische Rundschau,* **8** Jahrgang, Heft 1/2, 81–87.

Nilsson, E. D. 1996. Planetary boundary layer structure and air mass transport during the International Arctic Ocean Expedition 1991. *Tellus* **48B**, this issue.

Overland, J. E. and Guest, P. S. 1991. The Arctic snow and air temperature budget over sea ice during winter. *J. Geophys. Res.* **96**, C3, 4651–4662.

Shapiro, M. A. and Fedor, L.S. 1986. *The Arctic expedition 1984: Research aircraft observations of fronts and polar lows over the Norwegian and Barents sea*, Part 1. NOAA/ERL/Wavepropagation laboratory, Boulder CO 80303, USA, 56 pp.

Silverman, B. A. and Weinstein, A.I. 1974. *"Fog" weather and climate modification*, W. Hess (ed.). New York, John Wiley and Sons, p. 355.

Sverdrup, H. U. 1930a. *Norwegian north polar expedition 1918-1925, Meteorology*, Part I, *Discussion*, vol II. Geofysisk Institutt, Bergen, A. S. John Griegs boktryckeri.

Sverdrup, H. U. 1930b. *Norwegian north polar expedition 1918-1925, Meteorology*, Part II, *Tables*, vol. II. Geofysisk Institutt, Bergen, A. S. John Griegs boktryckeri.

Voskresensky, A. I. 1969. Mikrofizicheskaia struktura letnikh tumanov v Arktike. [*Microphysical structure of summer fogs in the Arctic.*] Leningrad Arkticheskii i Antarkticheskii Nauchno–Issledovatel'skii Institut, Trudy, 287, 69–80.

Vowinckel, E. and Orvig, S. 1962. Relation between solar radiation income and cloud type in the Arctic. *J. Applied. Met.* **1**, 552–559.

Vowinckel, E. and Orvig, S. 1970. The climate of the north polar basin, in climates of the polar regions, ed. S. Orvig. *World Survey of Climatology*, **14**.

Walter, B. A. and Overland, J. E. 1984. Observations of longitudinal rolls in a near neutral atmosphere. *Month. Weath. Rev.* **112**, 200–208.

Walter, B. A. and Overland, J. E. 1991. Aircraft observations of the mean and turbulent structure of the atmospheric boundary layer during spring in the central Arctic. *J. Geophys. Res.* **96**, C3, 4663–4673.